Stiffness Profiling of Pavement Subgrades

GLENN J. RIX AND KENNETH H. STOKOE II

The Spectral-Analysis-of-Surface-Waves (SASW) method is an in situ seismic method that permits detailed profiles of small-strain moduli to be determined at both soil and pavement sites. The method, which is nondestructive, is based on the dispersive characteristic of surface (Rayleigh) waves propagating in a layered medium. One of the principal advantages of this method is that all testing is performed on the ground surface. A second advantage for evaluating the properties of pavement systems is that the method can be used to determine the stiffness of the subgrade *before*, *during*, and *after* placement of the pavement system. These advantages are illustrated using a series of tests on a silty clay subgrade performed before and after placement of a concrete slab 10 in. (0.25 m) thick. A sensitivity study of the subgrade measurements and a method of characterizing nonlinear subgrade behavior are also presented.

Pavement subgrades can be investigated by a variety of in situ methods. However, the in situ method or combination of methods selected depends on factors such as the purpose of the investigation, the applicability of the method, and the availability of test equipment. When the subgrade is to be characterized by in situ moduli, seismic methods are the most direct in situ methods to use.

One seismic method, the Spectral Analysis of Surface Waves (SASW) method, is especially well suited for in situ investigation of pavement subgrades. An important feature of the SASW method is that it can be used either directly on the subgrade, on the base, or on the pavement surface layer at any time during the construction and subsequent life of the pavement. The SASW method is based on the generation and measurement of stress waves (Rayleigh waves) propagating along the surface. The propagation velocities of the Rayleigh wave are directly related to small-strain elastic moduli of the material through which they propagate. If moduli at larger strains are required, then in situ measurements of small-strain moduli are combined with laboratory and/or empirical results to describe the nonlinear behavior.

The purpose of this paper is to discuss the field and analysis procedures used in the SASW method. Results from one site where tests were performed directly on the subgrade and subsequently on a concrete slab cast on the subgrade are presented. The sensitivity of the measurements and the incorporation of nonlinear subgrade behavior are also discussed.

G. J. Rix, Department of Civil Engineering, Georgia Institute of Technology, Atlanta, Ga. 30332. K. H. Stokoe II, Geotechnical Engineering, The University of Texas at Austin, Austin, Tex. 78712-1076.

OVERVIEW OF SASW METHOD

The SASW method is an engineering seismic method that uses the dispersive property of surface waves to determine the shear modulus profile at soil sites and/or the Young's modulus profile at pavement sites. Several aspects of the SASW method make it particularly well suited for use by transportation engineers. The first two of these aspects are the method's nondestructiveness and nonintrusiveness. Both the source and the receivers are located on the ground surface, thereby eliminating the need for boreholes. Furthermore, because the source imparts only low-level stress waves, the testing is nondestructive. The third aspect is that the method can be used to test exposed subgrades as well as completed pavements.

The following sections briefly describe the dispersive behavior of surface waves in a layered half space and the test procedure used in SASW testing.

Surface Wave Dispersion

To understand how surface waves can be used to determine the modulus profiles of subgrades and pavements, it is first necessary to understand surface wave dispersion in a layered profile. A dispersive wave is one in which the velocity of propagation varies with frequency (which is the same as saying that velocity varies with wavelength). Surface wave dispersion is caused by the distribution of particle motion with depth. As wavelength increases, particle motion extends to greater depths in the profile, as illustrated in Figure 1. The velocities of surface waves are representative of the material properties over depths where there is significant particle motion. For example, the particle motion of a wave that has a wavelength less than the thickness of the pavement surface layer is confined to this layer (Figure 1b). Therefore, the wave velocity is influenced only by the properties of the surface layer. The velocity of a wave with a wavelength of several feet is influenced by the properties of the surface layer, base, and subgrade because a significant portion of the particle motion is in these layers (Figure 1c). Thus, by using surface waves over a wide range of wavelengths, it is possible to assess material properties over a range of depths.

The objective in SASW testing is to make field measurements of surface wave dispersion (i.e., measurements of surface wave velocity at various wavelengths) at soil and pavement sites and then to determine the shear wave velocities of the layers in the profile. These velocities can, in turn, be used

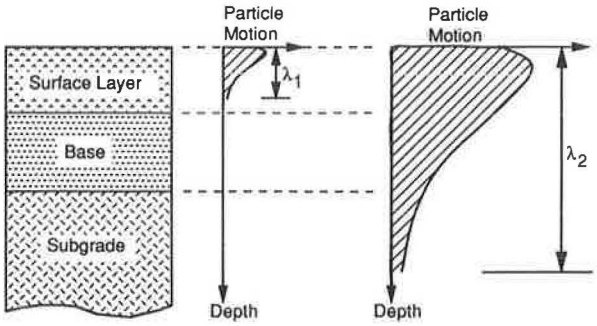

FIGURE 1 Approximate distribution of vertical particle motion with depth for two surface waves of different wavelengths.

to calculate values of shear and Young's moduli using simple relationships from the theory of elasticity.

SASW Test Procedure

The procedure used to perform an SASW test can be divided into three steps: (a) field testing, (b) dispersion calculations, and (c) inversion (*1*). In the following sections, a brief description of each of these steps is presented.

Equipment and Field Setup

The configuration of source, receivers, and recording equipment used in SASW testing is shown in Figure 2. The most common types of sources used to date have been simple hammers or dropped weights that strike the ground surface and create a transient wave containing a broad range of frequencies. Recently, however, the use of electromechanical vibrators to transmit random or sinusoidal input motions to the ground has also shown promise (*2*).

Selection of receivers is based on the range of frequencies

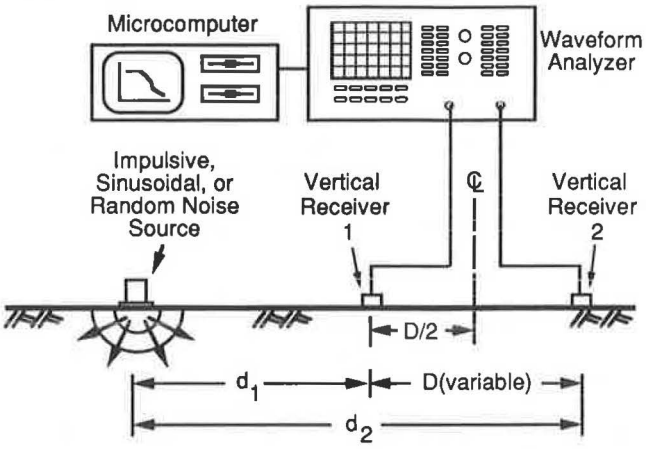

FIGURE 2 Configuration of equipment used in field testing.

that will be used to profile the site. For subgrade profiling where the objective is to develop a profile to approximately 10 ft (3 m), the frequencies range from approximately 50 to 1000 Hz. In this range of frequencies, geophones (velocity transducers) with a natural frequency of 4.5 Hz perform well. The geophones are coupled to the soil using spikes 2 in. (5 cm) long. For profiling concrete or asphaltic pavements, much higher frequencies (up to 50 kHz) are used to generate very short wavelengths so that the pavement surface layer can be evaluated. Piezoelectric accelerometers, coupled to the pavement with mounting wax (*3*), are typically used in this range of frequencies.

A dual-channel fast Fourier transform (FFT) analyzer is used to record and analyze surface wave motion at the two receivers. An essential feature of this type of instrument is the ability to perform frequency domain calculations (described subsequently) in real time. Finally, a microcomputer is used to transfer data from the analyzer and to perform the dispersion calculations described in the following section.

The spacing between receivers ($D = d_2 - d_1$ in Figure 2) varies according to the range of wavelengths used. In principle, it should be possible to use a single receiver spacing to perform an entire test. However, factors such as the attenuation of particle motion with horizontal propagation distance dictate that data from several different receiver spacings be combined for each test. For subgrade profiling, receiver spacings ranging from 1 to 16 ft (0.3 to 4.9 m) are typically used. For profiling the pavement surface layer and base materials, spacings of 0.25 to 4 ft (0.08 to 1.2 m) are employed. The distance from the source to the first receiver (d_1 in Figure 2) is usually equal to the distance between receivers (*1*, *4*).

The progression of receiver spacings at one site is illustrated in Figure 3. An imaginary centerline is established which remains fixed throughout the test. The receivers are placed equidistant from the centerline with the desired distance (D) between them (Figure 3a). This distance is related to the minimum wavelength that must be used to profile the near-

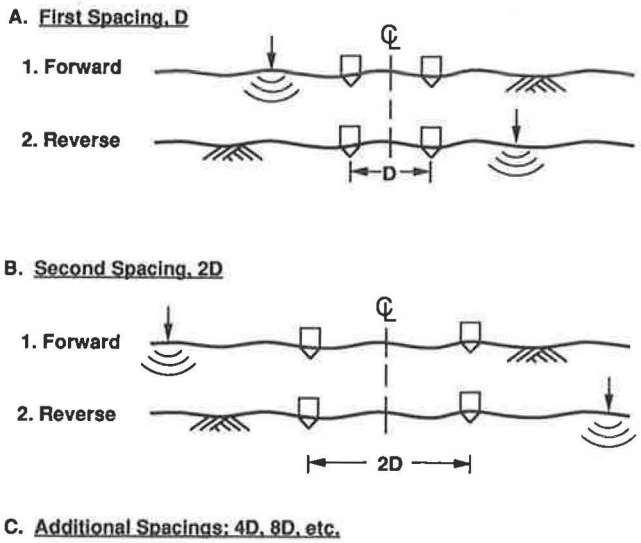

FIGURE 3 Arrangement of source and receivers illustrating the common midpoint geometry and forward and reverse tests at each receiver spacing.

surface layers. After the measurements described in the next section are performed at this spacing, the location of the source is reversed with respect to the geophones to perform a reverse profile (Figure 3a). (The results from reverse and forward profiling are compared to check data consistency and lateral homogeneity.) The distance between the receivers is then increased (typically doubled), and the measurements are repeated at the new spacing (Fig. 3b). Testing continues in this fashion until measurements at the maximum spacing have been completed. The maximum spacing is determined by the longest wavelength required to evaluate the shear wave velocity profile to a predetermined depth. For instance, if a profile to a depth of 10 ft (3 m) is desired, a maximum wavelength from 2 to 3 times this depth should be measured.

Dispersion Calculations

For each source-receiver spacing, surface waves are generated by striking the soil or pavement surface with a hammer or dropped weight or by using an electromechanical vibrator to transmit random or sinusoidal input motion to the ground surface. The time histories recorded by the two receivers, [$x(t)$ and $y(t)$] are transformed to the frequency domain, resulting in the linear spectra of the two signals [$X(f)$ and $Y(f)$]. The cross power spectrum of the signals [$G_{yx}(f)$] is then calculated by multiplying $Y(f)$ by the complex conjugate of $X(f)$. In addition to the cross power spectrum, the coherence function and the auto power spectrum of each signal are also calculated. It must be emphasized that all of these calculations are performed in real time by the FFT analyzer. The key data, consisting of the phase of the cross power spectrum and the coherence function, are shown in Figure 4. The coherence function represents a signal-to-noise ratio and should be nearly equal to 1 in the range of acceptable data (25 to about 150 Hz in Figure 4).

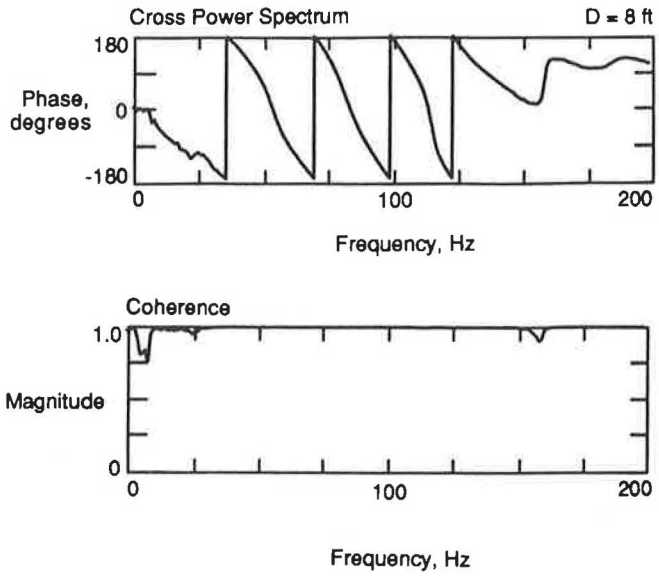

FIGURE 4 Spectral functions obtained using swept-sine input motion for a receiver spacing of 8 ft (2.4 m) on a silty clay subgrade.

The time delay between receivers as a function of frequency, denoted as $t(f)$, is calculated using the phase angle of the cross power spectrum, denoted as $\theta_{yx}(f)$, as follows:

$$t(f) = \theta_{yx}(f)/2\pi f \tag{1}$$

where the phase angle is in radians and the frequency (f) is in cycles/sec. The surface wave phase velocity (V_R) is determined using

$$V_R(f) = (d_2 - d_1)/t(f) \tag{2}$$

and the corresponding wavelength of the surface wave (L_R) is calculated from

$$L_R = V_R/f \tag{3}$$

These calculations give a dispersion curve (V_R versus L_R) for one receiver spacing. Individual dispersion curves are then combined to form the composite dispersion curve for the site. An example of a composite dispersion curve is presented in Figure 5 for SASW testing of a silty clay subgrade.

Inversion

Inversion is the process of calculating the shear wave velocity (or modulus) profile using the field dispersion curve. In the inversion process, a theoretical dispersion curve is calculated for an assumed velocity profile and is then compared to the field dispersion curve. The assumed velocity profile contains a sufficiently large number of sublayers to define the variation of material properties at the site. The theoretical curve is

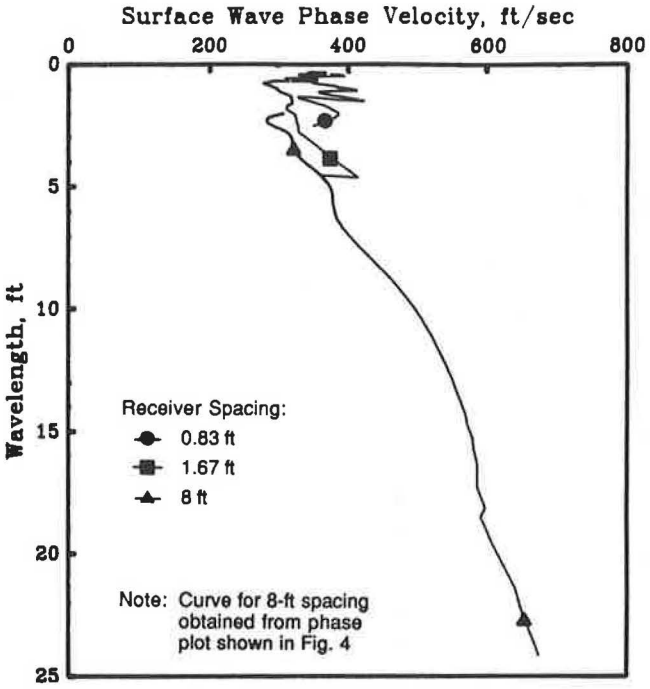

FIGURE 5 Composite dispersion curve for SASW testing of a silty clay subgrade.

calculated using a modified Haskell-Thomson matrix algorithm (*1*, *5*, *6*). The shear wave velocities and thicknesses of the sublayers in the assumed profile are adjusted by trial and error until a satisfactory match between the theoretical and field dispersion curves is obtained. Once a satisfactory match is obtained, the final profile is assumed to represent the actual site conditions. Application of inverse theory to surface wave testing has increased the accuracy of the resulting profiles and has expanded the variety of sites at which the SASW method can be used.

SITE DESCRIPTION

A series of tests was performed to demonstrate the use of the SASW method on both subgrades and pavement sites. These tests were conducted at the Hornsby Bend test site located in Austin, Texas. A description of the soil stratigraphy and properties is presented below, along with a description of the concrete slab constructed at the site.

Soil borings show four basic strata: (a) a silty clay layer extending from the surface to 13.5 ft (4.1 m), (b) a silty clay layer interbedded with silty fine sand seams from 13.5 to 33.5 ft (4.1 to 10.2 m), (c) a loose to medium-dense, silty fine sand layer from 33.5 to 45 ft (10.2 to 13.7 m), and (d) a hard gray clay layer extending from 45 ft (13.7 m) to the maximum depth of the borings, 50 ft (15.2 m). Undrained shear strengths over the depth range of 2 to 20 ft (0.6 to 6.1 m) estimated using a pocket penetrometer are greater than 3.0 kips/ft^2 (144 kPa).

A concrete test slab was cast directly on the silty clay subgrade after all vegetation was removed. The slab was unreinforced and had dimensions of 8 by 12 ft (2.4 by 3.7 m) with a nominal thickness of 10 in. (25.4 cm). Class S concrete with Type I cement and a maximum aggregate size of 0.75 in. (1.91 cm) was used for the slab. The average 28-day strength determined from cylinder tests was 6,470 psi (44.5 MPa). It is believed that this slab adequately modeled a full-sized, unreinforced (or simply reinforced) pavement slab [usually 12 by 20 ft (3.7 by 6.1 m)].

SUBGRADE PROFILING

SASW tests were performed directly on the silty clay subgrade prior to casting the slab. Three receiver spacings [0.83, 1.67, and 8 ft (0.25, 0.51, and 2.4 m)] were selected to provide data over a sufficient range of wavelengths to determine the velocity (modulus) profile to a depth of several feet. The composite dispersion curve presented in Figure 5 is the result of these measurements. The differences between the three individual dispersion curves in the wavelength range of 0.5 to 5 ft (0.15 to 1.5 m) is typical of variability often observed near the surface at soil sites. The variability at this site is most likely caused by lateral inhomogeneity and secondary structure in the silty clay.

The field dispersion curve was inverted using the procedure outlined in the section entitled "Inversion" to determine the shear wave velocity and Young's modulus profiles. The Young's modulus of each layer was derived from the shear wave velocity using the following relationship:

$$E = 2\rho V_s^2(1 + \nu) \quad (4)$$

where

E = Young's modulus,
ρ = mass density,
V_s = shear wave velocity, and
ν = Poisson's ratio.

In the absence of direct measurements, values for mass density and Poisson's ratio are normally assumed. Reasonable values for these two parameters fall within a relatively small range and do not significantly affect the calculated value of Young's modulus (*1*). In this study, however, measured values of mass density and Poisson's ratio were used.

The shear wave velocity and Young's modulus profiles for the subgrade are presented in Table 1. The values reported for the half space represent average values for the layers below 12 ft (3.7 m). The match between the composite dispersion curve shown in Figure 5 and the inverted profile given in Table 1 is shown in Figure 6. The theoretical curve agrees well with the trend of the experimental dispersion curves. However, the theoretical dispersion curve is very smooth in comparison with the experimental results and does not account for lateral variability. Until more sophisticated models of wave propagation are incorporated into inversion algorithms, it will not be possible to match the theoretical and experimental curves more exactly than is shown in Figure 6.

Finally, values of shear wave velocity determined from SASW testing are compared with those determined using an independent seismic method, the crosshole test, in Figure 7. The overall trends for the two methods are very similar, partic-

TABLE 1 VALUES OF SHEAR WAVE VELOCITY AND YOUNG'S MODULUS RESULTING FROM INVERSION OF SASW TESTS ON SILTY CLAY SUBGRADE

Layer No.	Layer Thickness (ft)	Shear Wave Velocity (ft/sec)	Young's Modulus (ksf)	Mass Density+ (lb-sec^2/ft^4)	Poisson's Ratio++
1	1.0	376	1259	3.4	0.31
2	1.0	339	1024	3.4	0.31
3	1.0	421	1531	3.4	0.27
4	1.0	559	2699	3.4	0.27
5	1.0	952	7642	3.4	0.24
6	1.0	943	7498	3.4	0.24
7	1.0	942	7482	3.4	0.24
8	1.0	817	5492	3.4	0.21
9	1.0	817	5492	3.4	0.21
10	1.0	860	6085	3.4	0.21
11	1.0	823	5711	3.4	0.24
12	1.0	905	6906	3.4	0.24
Half Space		1018	8738	3.4	0.24

+ Determined from the average of two undisturbed samples within the upper 4 ft

++ Determined from compression and shear wave velocities measured by crosshole seismic testing

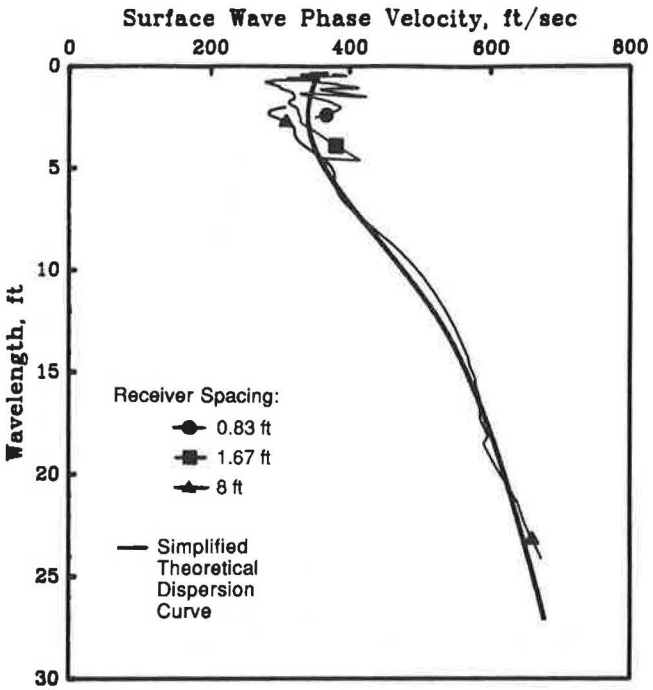

FIGURE 6 Comparison of theoretical and experimental dispersion curves for measurements of a silty clay subgrade.

ularly in light of the fact that the two tests were performed 2 years apart. Differing weather conditions (rainfall, temperature, etc.), lateral variability, and secondary soil structure are responsible for much of the difference between the results of the two test methods near the surface.

CONCRETE SLAB

Surface wave tests were also performed on the concrete slab following the same procedure used to profile the subgrade.

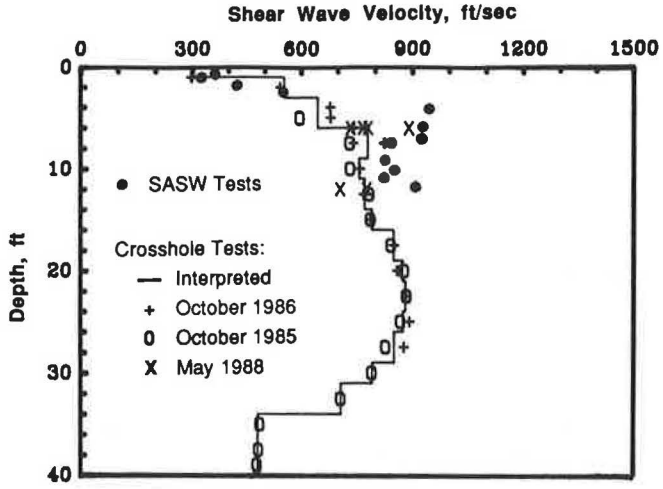

FIGURE 7 Shear wave velocity profiles from crosshole and SASW tests at the Hornsby Bend site.

In this test series, measurements were made during the time the concrete was curing so that the slab-subgrade system would appear to be many different systems, each with a different ratio of Young's modulus between the concrete and the soil. Receiver spacings of 0.83 and 1.67 ft (0.25 and 0.51 m) were used. Unfortunately, larger spacings could not be used due to the reduced size of the isolated slab.

Composite dispersion curves corresponding to two measurement times during curing of the slab are presented in Figure 8. The first curve (Figure 8a) results from measurements made approximately 5 hours after the addition of water to the cement-aggregate mixture. The curing process was actively proceeding at this time. This point is supported by the relatively low values of surface wave velocity [approximately 4,000 fps (1220 m/s)] measured at short wavelengths [less than 0.83 ft (0.25 m)] in the concrete. Fluctuations in the dispersion curves, particularly between wavelengths of 1.5 and 2 ft (0.45 to 0.6 m), are caused by reflections of waves

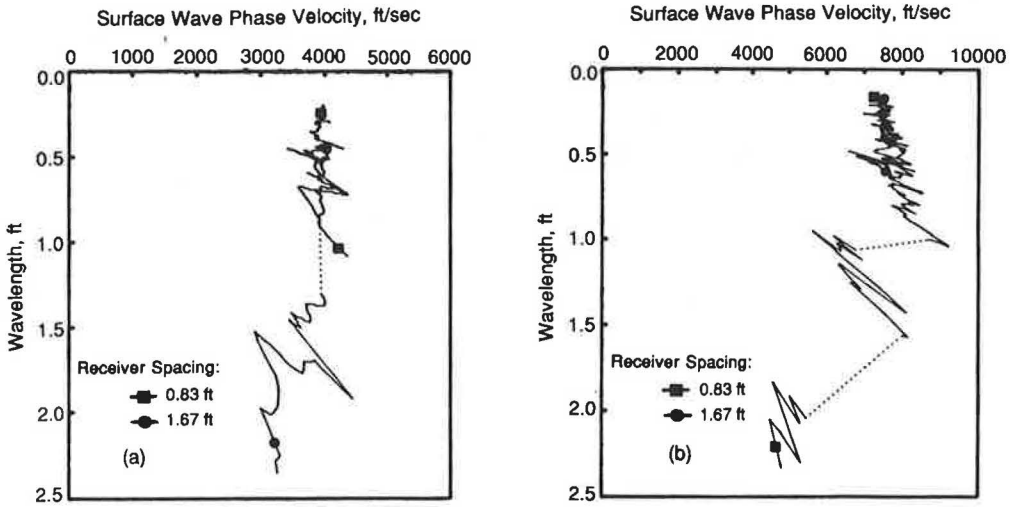

FIGURE 8 Dispersion curves for measurements on slab-subgrade system initiated (a) 5 hours and (b) 4 days after the addition of water to the cement-aggregate mixture.

from the lateral and bottom boundaries of the slab. The dotted line in Figure 8a represents a gap in the dispersion curve caused primarily by interference from reflecting waves (*3*).

The composite dispersion curve in Figure 8b corresponds to measurements made after 4 days, when the concrete was more fully cured. Measured surface wave velocities now range between 7,000 and 8,000 fps (2135 to 2440 m/s), which is a typical range for cured concrete. As with the earlier measurements, reflections from the lateral and bottom boundaries of the slab have caused fluctuations and gaps in the composite dispersion curve (as discussed subsequently in this section). It is important to note, however, that the dispersion curves in Figure 8 exhibit nearly constant values of phase velocity for wavelengths less than the thickness of the slab [0.83 ft (0.25 m)]. This behavior permits the modulus and the thickness of the pavement surface layer to be determined rapidly and without the need for inversion (*3*).

To demonstrate that surface wave measurements remain sensitive to the properties of the subgrade even in the presence of the slab, a comparison between theoretical and field dispersion curves is presented in Figure 9. This approach is followed rather than inversion of the measured dispersion curve shown in Figure 8b because the dimensions of the isolated slab did not permit measurement of sufficiently long wavelengths to use the inversion algorithm. The theoretical dispersion curve was calculated using a simplified subgrade profile, given in Table 2, supporting a concrete pavement layer of infinite lateral extent. The profile in Table 2 was simplified from the more detailed profile reported in Table 1 so that the computational effort could be reduced. The shear wave velocity assigned to the concrete was determined in the field using an independent seismic method, and the nominal thickness of the slab was used. The algorithm used to calculate the theoretical dispersion curve (*4*) differs from that normally used for inversion (*1*) in that it models more completely wave propagation in a layered profile of infinite lateral extent (at the expense of significantly more computational effort).

A comparison of the experimental and theoretical dispersion curves is shown in Figure 9. The more complete algorithm used to calculate the theoretical curve models many of the features observed in the experimental curve, especially the large excursion in the wavelength range from 0.8 to 1.4 ft (0.24 to 0.43 m). This feature is caused by body waves reflecting from the bottom of the concrete slab. The decrease in phase velocity with increasing wavelength at wavelengths longer than 1.4 ft (0.43 m) shows that surface wave measurements remain sensitive to the properties of the subgrade in the presence of the pavement surface layer. This effect would have been more clearly demonstrated if measurement of longer wavelengths had not been precluded by the lateral dimensions of the slab.

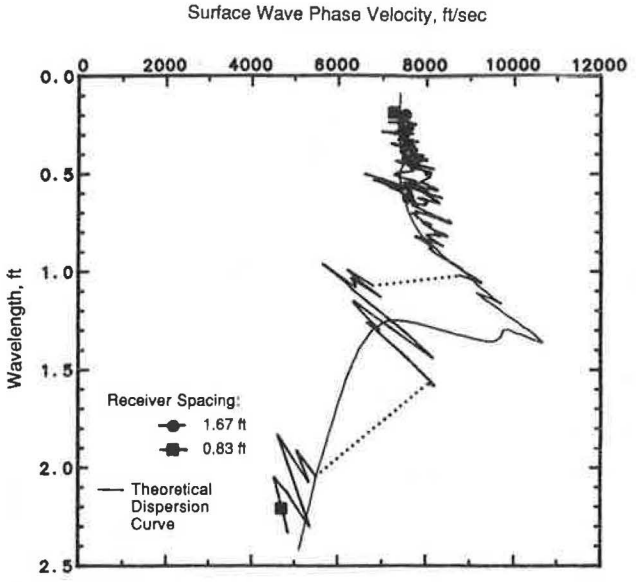

FIGURE 9 Comparison of field and theoretical dispersion curves for measurements on the slab-subgrade system.

To illustrate the influence of the lateral slab boundaries on these measurements, the algorithm used to calculate the theoretical dispersion curve in Figure 9 (*4*) was modified to include the effects of reflected surface waves from the four edges of the slab following the procedure presented by Sheu (*3*). This theoretical dispersion curve is presented in Figure 10. For comparison purposes, the theoretical dispersion curve presented in Figure 9 for wave measurements of a slab-subgrade system of infinite lateral extent is also included. One can see that inclusion of the lateral boundaries results in the theoretical dispersion curve modelling essentially all of the features exhibited in the experimental curve (Figure 9). The comparison also indicates the extent to which the use of a more complete theoretical algorithm can improve surface wave testing by more accurately modelling field conditions. It is to be hoped that the computational effort needed for these algorithms can be reduced in the future so that they can be used in routine tests.

SENSITIVITY STUDY

One of the questions often raised about the results obtained using the SASW method is the sensitivity of the inversion

TABLE 2 SIMPLIFIED PROFILE OF SILTY CLAY SUBGRADE USED IN ANALYTICAL STUDIES SHOWN IN FIGURES 9–13

Layer No.	Layer Thickness (ft)	Shear Wave Velocity (ft/sec)	Young's Modulus (ksf)	Mass Density (lb-sec^2/ft^4)	Poisson's Ratio
1	2	355	1,123	3.4	0.31
2	1	420	1,523	3.4	0.27
3	1	560	2,708	3.4	0.27
4	3	945	7,530	3.4	0.24
Half space		850	5,945	3.4	0.22

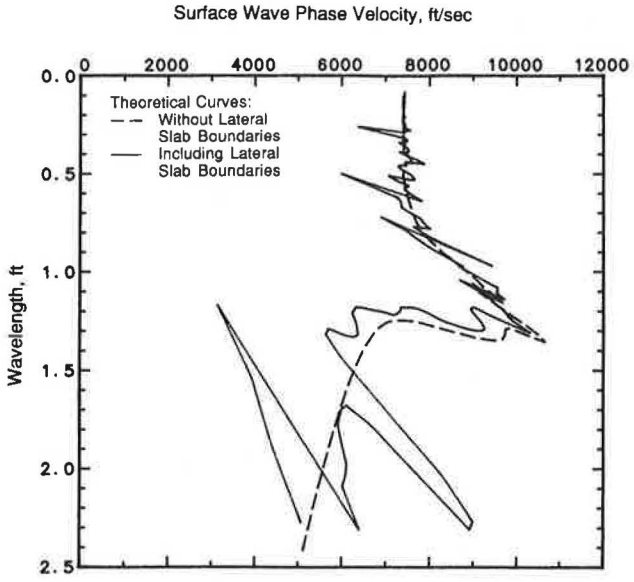

FIGURE 10 Influence of lateral slab boundaries on the theoretical dispersion curve of the slab-subgrade system.

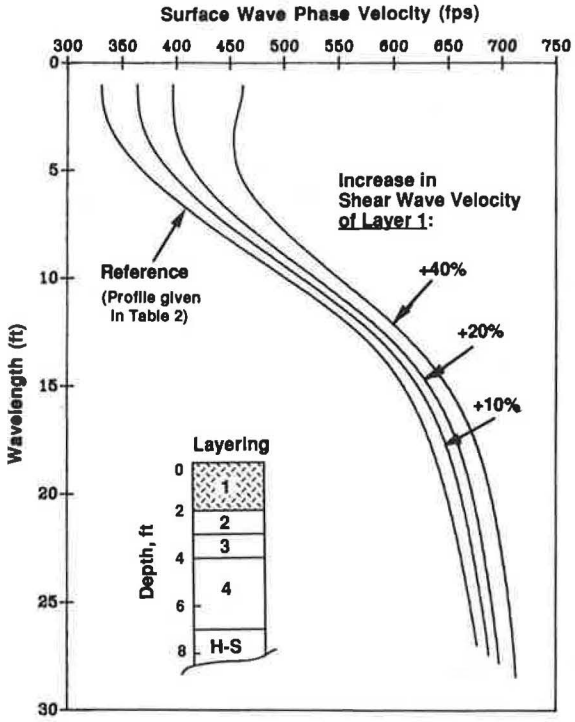

FIGURE 11 Variations in the theoretical dispersion curve resulting from increasing the velocity of Layer 1 in the subgrade.

procedure. More specifically, it is desirable to estimate the resolution of the final shear wave velocity and Young's modulus profiles. A preliminary analytical study of this question was performed on the subgrade measurements using the simplified profile presented in Table 2.

Initially, the shear wave velocity of the top layer was increased by 10, 20, and 40 percent, and theoretical dispersion curves were calculated for each altered profile. (Changes of 10, 20, and 40 percent in the shear wave velocity of a layer correspond to changes of 21, 44, and 96 percent in the Young's modulus of the layer.) These "perturbed" dispersion curves are shown in Figure 11. Clearly, the shear wave velocity of the top layer exerts a large influence on the dispersion curve. Part of the reason for this large influence is that the thickness of the top layer [2 ft (0.61 m)] is a significant portion of the total depth (not including the half space) of the profile [7 ft (2.1 m)]. The large differences between the dispersion curves at short wavelengths [less than 3 ft (0.9 m)] imply that the shear wave velocity of the first layer can be resolved very accurately because shear wave velocities for the first layer which differ by as little as 10 percent shift the entire curve by an amount that results in an unsatisfactory match with the field dispersion curve. However, as illustrated in Figure 5, it is often the lateral variability at the site that controls the accuracy with which the stiffness of the top layer can be determined, rather than the resolving power of the SASW method.

The results of increasing the shear wave velocity of the second layer by 10, 20, and 40 percent are shown in Figure 12. The differences between the perturbed and unperturbed dispersion curves are less pronounced in this case. One reason is that the thickness of Layer 2 represents a smaller fraction of the total thickness of the profile than the thickness of Layer 1. The dispersion curve corresponding to an increase of 10 percent is sufficiently similar to the unperturbed curve that, in the writers' experience, a satisfactory match would likely result when considering normal site variability. An increase

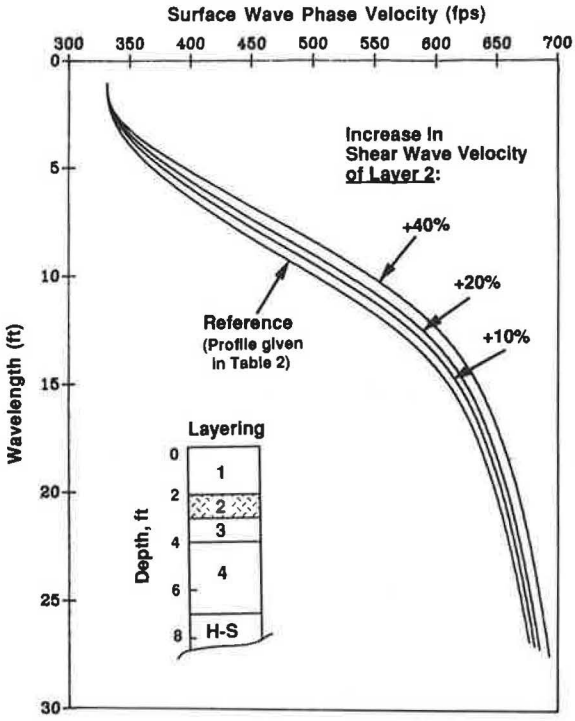

FIGURE 12 Variations in the theoretical dispersion curve resulting from increasing the velocity of Layer 2 in the subgrade.

of 20 percent in the velocity of Layer 2 changes the dispersion curve by an amount that results in an unsatisfactory match with the field dispersion curve (Figure 5). In fact, this shift would likely result in a poor match with most field dispersion curves. Finally, a 40-percent increase in the shear wave velocity of Layer 2 produces a significant change in the dispersion curve, which further heightens the mismatch between the theoretical and field dispersion curves.

Results similar to those for variations in Layer 2 were also found for Layers 3 and 4 (7). As one would intuitively expect from an understanding of surface wave dispersion, changes in the shear wave velocity of the subgrade layers result in smaller differences between perturbed and unperturbed dispersion curves as layer depth increases and as layer thickness decreases. However, changes in shear wave velocities greater than 20 percent at this site resulted in unsatisfactory matches between theoretical and field dispersion curves.

The final comparison performed in the sensitivity study was that of "compensating" changes in wave velocities of adjacent layers. This comparison was done by increasing the shear wave velocity of Layer 2 by 20 percent and decreasing the velocity of Layer 3 by 25 percent. As shown in Figure 13, the perturbed dispersion curve differs from the unperturbed curve in two respects: (a) in the slope over wavelengths from 5 to 15 ft (1.5 to 4.6 m) and (b) in wave velocities over wavelengths from approximately 10 to 20 ft (3.1 to 6.1 m). As a result of these two differences, the perturbed dispersion curve does not satisfactorily match the field dispersion curve. In the writers' experience, potential errors caused by compensating changes can be avoided, especially for layers near the surface.

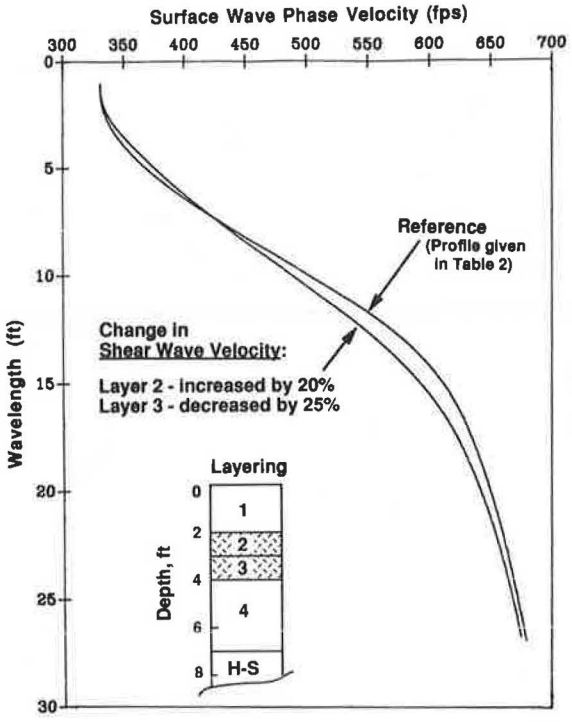

FIGURE 13 Variation in the theoretical dispersion curve resulting from "compensating" changes in subgrade layer velocities.

NONLINEAR SUBGRADE BEHAVIOR

The evaluation of subgrade moduli from the measurement of propagation velocities of stress waves, as done in seismic tests, results in the determination of small-strain elastic moduli. These moduli characterize the deformational behavior of subgrade in the range of strain where linear, elastic behavior is valid (typically at axial strains less than 0.001 percent). As illustrated in Figure 14, these moduli represent the initial slope of the stress-strain curve. The term *initial tangent modulus* is often used to refer to small-strain moduli that are commonly denoted as E_0 or E_{max}. Moduli determined at higher levels of strain, where linear behavior in subgrade soils is no longer valid, are secant moduli and are denoted by E_1, E_2, etc., as shown in Figure 14.

To study the nonlinear behavior of the silty clay subgrade, undisturbed samples were taken, and torsional resonant column tests were performed. Initial tangent and secant moduli determined from one sample at four different confining pressures are shown in Figure 15. The constant value of Young's modulus at strains less than about 0.001 percent is clearly shown. To estimate nonlinear behavior in situ, the curves are first normalized with respect to the initial tangent modulus, as shown in Figure 16. The in situ modulus at any strain is then determined by multiplying the in situ modulus from the field seismic measurements by the normalized value of the

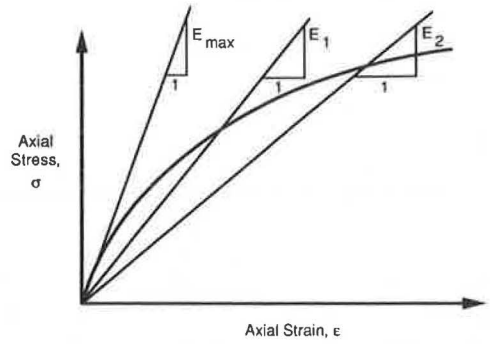

FIGURE 14 Characterization of nonlinear soil behavior by initial tangent (E_{max}) and secant (E_1, E_2, etc.) Young's moduli.

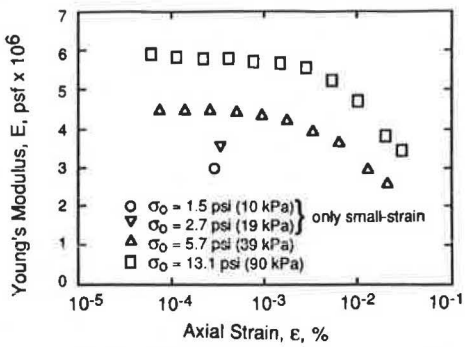

FIGURE 15 Variation in Young's modulus with strain amplitude of the silty clay subgrade.

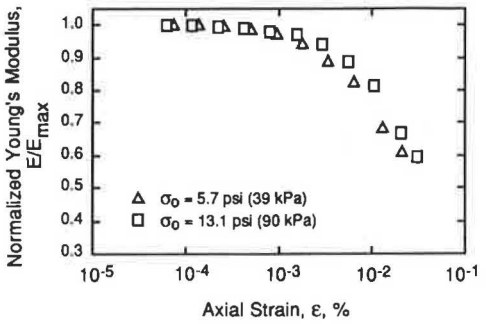

FIGURE 16 Variation in normalized Young's modulus with strain amplitude of the silty clay subgrade.

modulus from the laboratory test at the desired strain. This procedure can be written as:

$$E_{\varepsilon,\text{field}} = E_{\text{seismic}} \cdot (E_\varepsilon/E_{\max})_{\text{lab}} \quad (5)$$

where

E_{seismic} = small-strain modulus determined in situ,
$(E_\varepsilon/E_{\max})_{\text{lab}}$ = normalized modulus determined by cyclic laboratory test at a strain amplitude of ε, and
$E_{\varepsilon,\text{field}}$ = modulus in the field at a strain amplitude of ε.

For instance, if Young's modulus at a depth of 1.5 ft (0.45 m) and an axial strain of 0.01 percent is needed, the modulus from the seismic measurement (1,024 ksf in Table 1) is multiplied by 0.75. (The multiplier could be slightly reduced to about 0.70 if the confinement level was significantly lower than that used in the test.) This general approach is the same as that used in geotechnical earthquake engineering to evaluate nonlinear soil response during earthquake shaking (*8*).

CONCLUSIONS

The SASW method can be used to assess the moduli of individual layers within a pavement profile at small-strain levels (< 0.001 percent) where the behavior of pavement materials is linear and elastic. An advantage of the SASW method is that it can be used to determine the modulus profile at any time during the construction and subsequent life of the pavement. Two series of tests were performed which illustrate the use of the method directly on subgrade soils and on a completed pavement. The results of these tests indicate that the SASW method remains sensitive to the subgrade properties despite the presence of the pavement surface layer.

A sensitivity study was performed on the subgrade tests to quantify the resolving power of the SASW measurements. The study revealed that the modulus of the top layer was determined within about 10 percent of the in situ value, whereas the moduli of other near-surface layers were determined within about 10 to 30 percent. One important characteristic of any site is lateral variability, which decreases the resolving power of the SASW method as variability increases. Finally, a method of characterizing nonlinear subgrade behavior by combining small-strain moduli determined in situ using seismic methods with experimental (or empirical) modulus degradation curves is presented for the silty clay subgrade.

ACKNOWLEDGMENTS

This work was supported by the Texas State Department of Highways and Public Transportation. The authors wish to express their appreciation for this support. The authors also wish to thank D.-W. Chang and J. A. Bay for their assistance with some of the analytical studies and R. D. Andrus and D.-S. Kim for conducting the resonant column tests.

REFERENCES

1. S. Nazarian. *In Situ Determination of Elastic Moduli of Soil Deposits and Pavement Systems by Spectral Analysis of Surface Waves Method*. Ph.D. dissertation. University of Texas at Austin, 1984, 453 pp.
2. G. J. Rix. *Experimental Study of Factors Affecting the Spectral Analysis of Surface Waves Method*. Ph.D. dissertation. University of Texas at Austin, 1988, 315 pp.
3. J.-C. Sheu. *Applications and Limitations of the Spectral Analysis of Surface Waves Method*. Ph.D. dissertation. University of Texas at Austin, 1987, 280 pp.
4. I. Sanchez-Salinero. *Analytical Investigation of Seismic Methods Used for Engineering Applications*. Ph.D. dissertation. University of Texas at Austin, 1987, 401 pp.
5. N. A. Haskell. The Dispersion of Surface Waves in Multilayered Media. *Bulletin of the Seismological Society of America*, Vol. 43, 1953, pp. 17–34.
6. W. T. Thomson. Transmission of Elastic Waves through a Stratified Solid. *Journal of Applied Physics*, Vol. 21, 1950, pp. 89–93.
7. G. J. Rix, K. H. Stokoe II, and J. M. Roesset. *Experimental Study of Factors Affecting the SASW Method*. Research Report 1123-1. Texas State Department of Highways and Public Transportation, forthcoming.
8. F. E. Richart, Jr., D. G. Anderson, and K. H. Stokoe II. Predicting In-Situ Strain-Dependent Shear Moduli. *Proc., 6th World Conference on Earthquake Engineering*, New Delhi, India, 1977, pp. 118–121.

Publication of this paper sponsored by Committee on Soil and Rock Properties.